Molecular Crystals and Liquid Crystals
Publication details, including instructions for authors and subscription information:
http://www.tandfonline.com/loi/gmcl16

Investigation of Structure and Dynamics in the Fibre-Type Nematic Phase of nBABA

K. Usha Deniz [a b], G. Pepy [a], P. Keller [a], B. Farnoux [a] & G. Parette [a]

[a] Laboratoire Léon Brillouin, CEN-SACLAY, 91191, GIF-SUR-YVETTE, Cédex, FRANCE

[b] Nuclear Physics Division, Bhabha Atomic Research Centre, Bombay, 400085, India

Version of record first published: 17 Oct 2011.

To cite this article: K. Usha Deniz , G. Pepy , P. Keller , B. Farnoux & G. Parette (1985): Investigation of Structure and Dynamics in the Fibre-Type Nematic Phase of nBABA, Molecular Crystals and Liquid Crystals, 127:1, 81-101

To link to this article: http://dx.doi.org/10.1080/00268948508080833

Mol. Cryst. Liq. Cryst., 1985, Vol. 127, pp. 81–101
0026-8941/85/1274–0081/$25.00/0

Printed in the United States of America

Investigation of Structure and Dynamics in the Fibre-Type Nematic Phase of nBABA†

K. USHA DENIZ‡, G. PEPY, P. KELLER, B. FARNOUX and G. PARETTE

Laboratoire Léon Brillouin, CEN-SACLAY, 91191 GIF-SUR-YVETTE Cédex, FRANCE

(*Received September 3, 1984*)

Neutron diffraction measurements have been carried out with chain deuterated (D-) and non-deuterated (H-) compounds, *p-n*-AlkoxyBenzylidene-*p*-Amino Benzoic Acids (nBABA, $n = 1, 3, 4$ and 7) in the fibre-type nematic (N_F) phase. For $n = 3$ and 4, our results indicate the presence of strings of one dimensional (1-*d*) correlated molecules parallel to $\hat{\mathbf{n}}$, the nematic director. The number of strings as well as the correlation length, $\xi_\perp^1$, perpendicular to $\hat{\mathbf{n}}$, decrease rapidly with increasing temperature. However, $\xi_\parallel^1$, the correlation length parallel to $\hat{\mathbf{n}}$, remains almost constant for $T_{PN} \leqslant T < T_{PN} + 30°C$ (T_{PN} = crystal to nematic transition temperature), but decreases for larger T. Neutron quasi-elastic scattering experiments carried out with 4BABA (both D- and H-) in the N_F phase have shown that, (a) the rotational diffusion times, τ_1^r and τ_1^f, for the rigid and flexible parts of the molecule, are not very different, and are $\sim 10^{-11}$s for $T \approx T_{PN}$, and (b) these motions are not influenced greatly by the 1-*d* correlation of the molecules.

INTRODUCTION

The compounds, *p-n*-AlkonyBenzylidene-*p*-Amino Benzoic Acids (nBABAs), C_nH_{2n+1}—O— 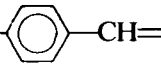 —CH=N— 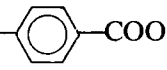 —COOH, exhibit[1] fibre-type nematic (N_F) phases which are characterized by two types of short range order (SRO), (Figure 1), namely (a) one-dimensional correlation along the nematic director, $\hat{\mathbf{n}}$ and (b) an S_c-

†Paper presented at the 10th International Liquid Crystal Conference, York, 15th–21st July 1984.

‡Present address: Nuclear Physics Division, Bhabha Atomic Research Centre, Bombay-400085, India.

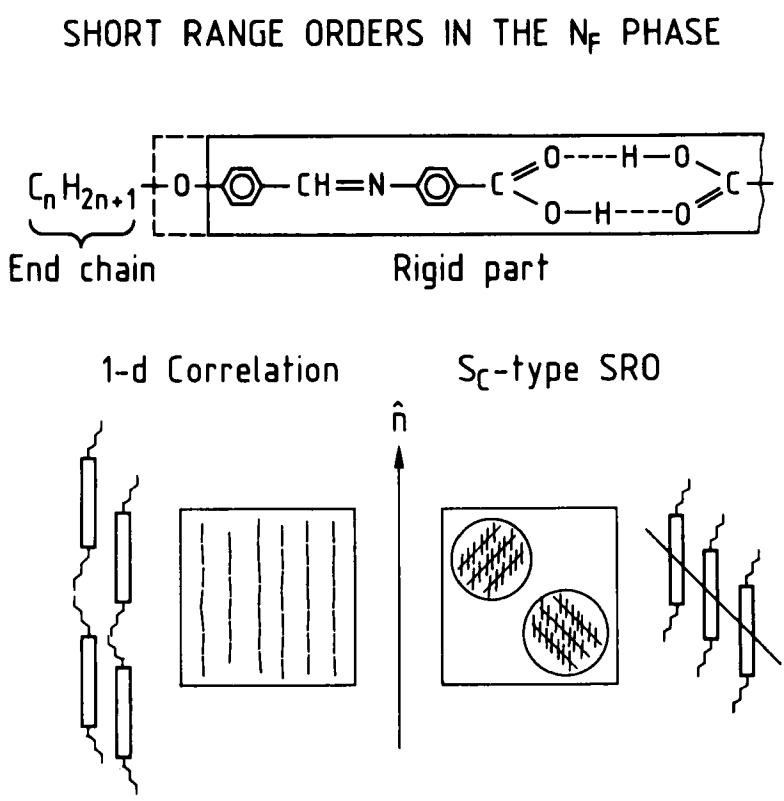

FIGURE 1 Schematic representation of the two types of short range orders (SRO) in the fibre type nematic (N_F) phase of nBABAs. The rigid part of the molecule includes the Oxygen atoms (dashed line).

type SRO as in the case of skewed cybotactic nematics.[2] A typical X-ray diffraction pattern obtained from a fibre-type nematic is shown schematically in Figure 2. The meridional lines (scattering vector, $\vec{\mathbf{Q}} \| \hat{\mathbf{n}}$) are due to one-dimensional (1-d) correlations of the molecules (i.e., strings), while the diffuse spots originate from the S_c-type SRO. The equatorial ($\vec{\mathbf{Q}} \perp \hat{\mathbf{n}}$) diffuse maxima are related to the molecular packing perpendicular to $\hat{\mathbf{n}}$. X-ray diffraction experiments[1] have shown that (1) the nBABA molecules exist as dimers in the nematic phase, (2) the strength of the 1-d correlation increases as n (the end chain length) increases from 1 to 4, but decreases for further increase of n, becoming negligible for $n = 7$, and (3) the S_c-type SRO which is very weak for $n \leq 3$, increases with increasing n. Calorimetric studies[3] have shown that the transition entropy (ΔS_{NI}), of the nematic to isotropic transition is quite large when compared to that of ordinary

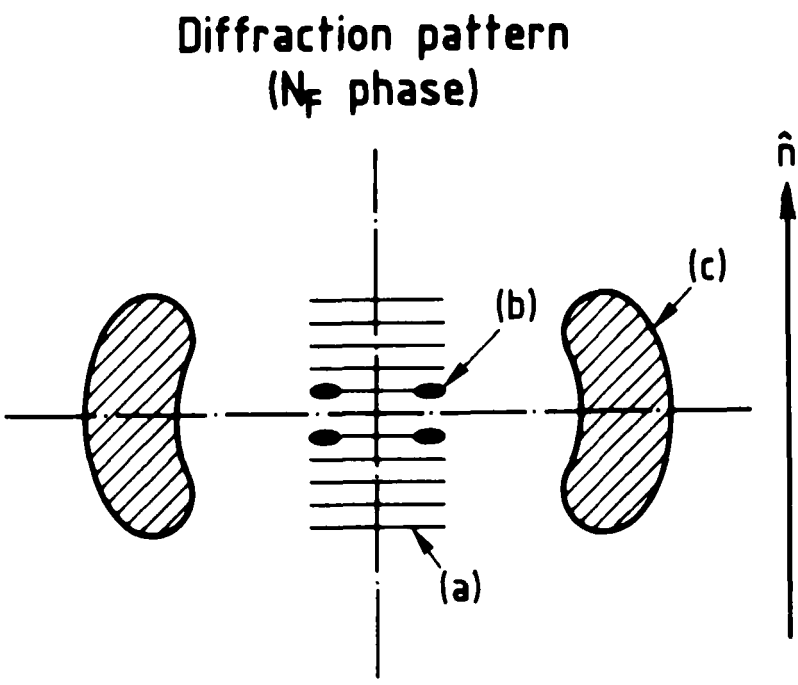

FIGURE 2 Schematic diagram of the diffraction pattern from an N_F phase. (a) Meridional lines, (b) Cybotactic spots and (c) Equatorial diffuse maxima. Most of the scans in the present work have been carried out along the dashed lines.

nematics. Since ΔS_{NI} is maximum for $n = 4$, just as it is for the strength of the 1-d correlation, it was speculated that perhaps the breaking down of the 1-d correlation is responsible for the high value of ΔS_{NI}.

In this paper we describe the results of neutron scattering experiments carried out with nBABAs ($n = 1, 3, 4$ and 7) in the N_F phase. Neutron diffraction measurements were carried out with these compounds in order to follow the evolution of the 1-d correlation as a function of n and of the temperature, T. Neutron quasielastic scattering (NQES) experiments were carried out with 4BABA to determine whether the structures resulting from the short range orders had any special effect on the rotational diffusion movements of the molecules. Chain deuterated compounds (D-nBABA) and non-deuterated (H-nBABA) compounds were used in both types of experiments so as to (a) obtain a better understanding of the molecular conformation and (b) separate the chain movements from those of the rest of the molecule. The experimental results shed light on the

molecular packing in the N_F phase. We have tried to explain our observations using models of molecular conformation and dynamics.

EXPERIMENTAL DETAILS

All our measurements were carried out at the ORPHEE reactor. The sample was always a monodomain nematic, with the molecules oriented by a magnetic field **H**, where $\mathbf{H} > 3$ K Oersteds in the case of the diffraction studies, and $\mathbf{H} = 1.3$ K Oersteds in the NQES experiments. The scattering vector $\vec{\mathbf{Q}}$ was almost always maintained either $\|\hat{\mathbf{n}}(\|\vec{\mathbf{H}})$ or $\perp\hat{\mathbf{n}}(\perp\vec{\mathbf{H}})$ (see dashed lines in Figure 2).

The diffraction work was carried out on three different spectrometers. The diffuse equatorial maximum was studied using the DNPX spectrometer having a banana-type multidetector. A vertical magnetic field was used and the scans were performed with $\vec{\mathbf{Q}}\perp\hat{\mathbf{n}}(Q_\perp)$. The incident wavelength, λ_0 was 4.775 Å. The double axis spectrometer, 4F2, with $\lambda_0 = 4.054$ Å was used for scanning the meridional lines. $\vec{\mathbf{H}}$ was horizontal and $\vec{\mathbf{Q}}\|\hat{\mathbf{n}}(Q_\|)$ for these scans. The small angle scattering spectrometer, PAXY, with the XY detector was used with $\lambda_0 = 3.12$ Å, for carrying out $\vec{\mathbf{Q}}\perp\hat{\mathbf{n}}$ scans along the sharp (2nd order) meridional line.

NQES experiments were performed on the triple axis spectrometer, 4F1, with $\lambda_0 = 4.488$ Å and a resolution of 2.10^{10} Hz ($\approx$80 μeV). The energy distributions were obtained for Q equal to 0.6 $Å^{-1}$ and 1.0 $Å^{-1}$. At each temperature at which energy distributions were studied, it was verified that the Q values did not fall within the domain in which the equatorial diffuse maximum occurred.

The lowest temperature at which the experiments were performed for each sample was about 0.5°C to 1.0°C above the transition temperature, T_{PN} (where P is a crystalline phase for $n = 1, 3$ and 4 but is a S_c phase for $n = 7$). This temperature was arrived at by heating the sample to about T_{PC} + 5°C and cooling it to the desired temperature. The rest of the temperatures were obtained by heating the sample. In all the hydrogenous samples, except H-7BABA, the values of T_{PN} were within 1 or 2°C of the corresponding ones given by DSC. The deuterated samples had values of T_{PN}, which were about 2°C lower than those for the corresponding hydrogenous samples. The transition temperature for all samples decreased by about 2°C, after long use, showing a slight deterioration of the sample. We are not able to account for the large ($\approx$10°C) difference between T_{PN}(DSC) and T_{PN}(neutrons) for 7BABA. The temperature stability was better

than ± 0.5°C for all measurements. The compounds were always recrystallized from ethanol before being used.

RESULTS AND DISCUSSION

a. Equatorial scans:

The equatorial scans on DNPX reveal the existence of only one diffuse peak in the range, $0.7\ \text{Å}^{-1} \leq Q \leq 2.0\ \text{Å}^{-1}$. The diffuse peaks observed at 184.4°C and 254.5°C in the case of D-4BABA are shown in Figure 3. The peak which is at 1.40 Å^{-1} at 184.4°C, with a full width at half maximum (FWHM) of 0.35 Å^{-1}, shifts to 1.36 Å^{-1} at the higher temperature with a FWHM of 0.44 Å^{-1}. The peak position, width, and their temperature dependence are similar in all the compounds we have studied. Using the expression given by De Vries,[2] we have obtained, D, the intermolecular (or interstring) separation, $\perp \hat{\mathbf{n}}$. D

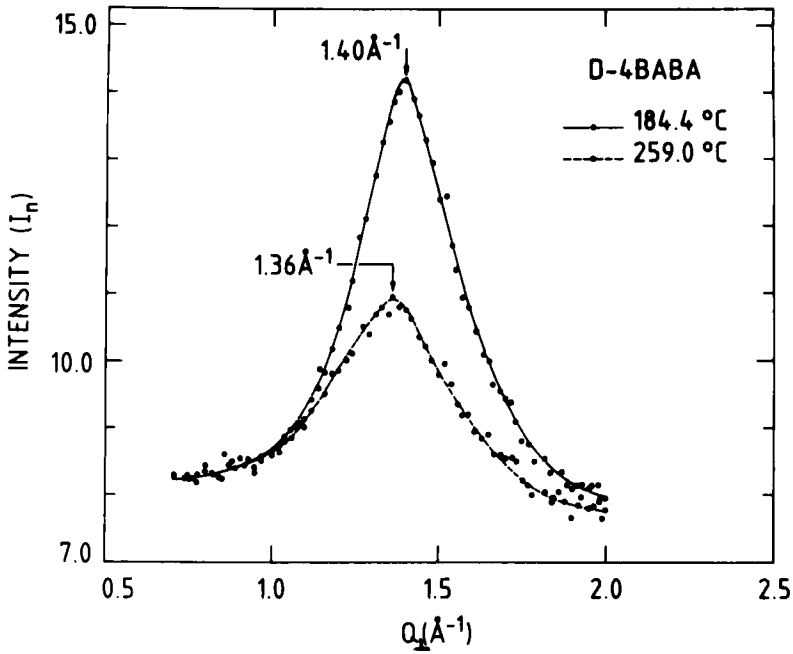

FIGURE 3 Normalised intensity, I_n, as a function of $Q_\perp$ ($\vec{\mathbf{Q}}_\perp \hat{\mathbf{n}}$) for the equatorial scan for D-4BABA.

changes from 4.95 Å at 184.4°C to 5.23 Å at 254.5°C. Although the observed width of the diffuse peak cannot be simply related to any particular correlation length,[4] it would be related to the correlation lengths of both, individual molecules and the 1-*d* correlated strings.[5] We can obtain such a correlation length, $L_\perp$, using Scherrer's equation:[5]

$$L_\perp = \frac{\lambda_0}{\beta_{1/2} \cos\theta} = \frac{4\pi}{\Delta Q} \tag{1}$$

where 2θ is the scattering angle, $\beta_{1/2}$ is the angular half-width of the peak, and ΔQ the FWHM of the peak in units of $Å^{-1}$. We obtain for $L_\perp$, values of 36 Å and 28 Å for the two temperatures. Since we know from the present work, that 1-*d* strings no longer exist at the higher temperature, this would imply a correlation length of 28 Å for the individual molecules $\perp \hat{\mathbf{n}}$. This value implies a correlation extending up to 5th nearest neighbours which seems somewhat large for the case of nematics. Perhaps, Scherrer's equation is not applicable in this case. If one uses an Ornstein-Zernike[6] type correlation function, the correlation length would be

$$L_\perp = \frac{2}{\Delta Q}$$

and this gives correlation lengths of about 6 Å and 5 Å for the two temperatures. In this case, the correlation extends up to only the 1st nearest neighbours, which seems reasonable.

b. Meridional scans ($\vec{\mathbf{Q}} \| \hat{\mathbf{n}}$)

Figure 4 shows the meridional scans ($\vec{\mathbf{Q}} \| \hat{\mathbf{n}}$) for the four deuterated compounds, for $T \approx T_{PN}$. The meridional distributions reveal several interesting features. (1) For $n = 3$ and 4, a number of diffraction peaks are found both in the H- and D-compounds, one of them being very intense and sharp. For $n = 1$ and 7, the number of peaks is less (see Table I) and no intense sharp peak is observed. In this respect, the neutron and X-ray diffraction results are similar. (2) The presence of the 1-*d* correlated strings of molecules is evidenced by the presence of the intense sharp peak and a decrease of the scattered intensity for small Q values. The sharp peak corresponds to a second order layer reflection due to 1-*d* correlated units, whose length, L_{cu}, is nearly equal to that of the molecular dimer. In the case of 7BABA,

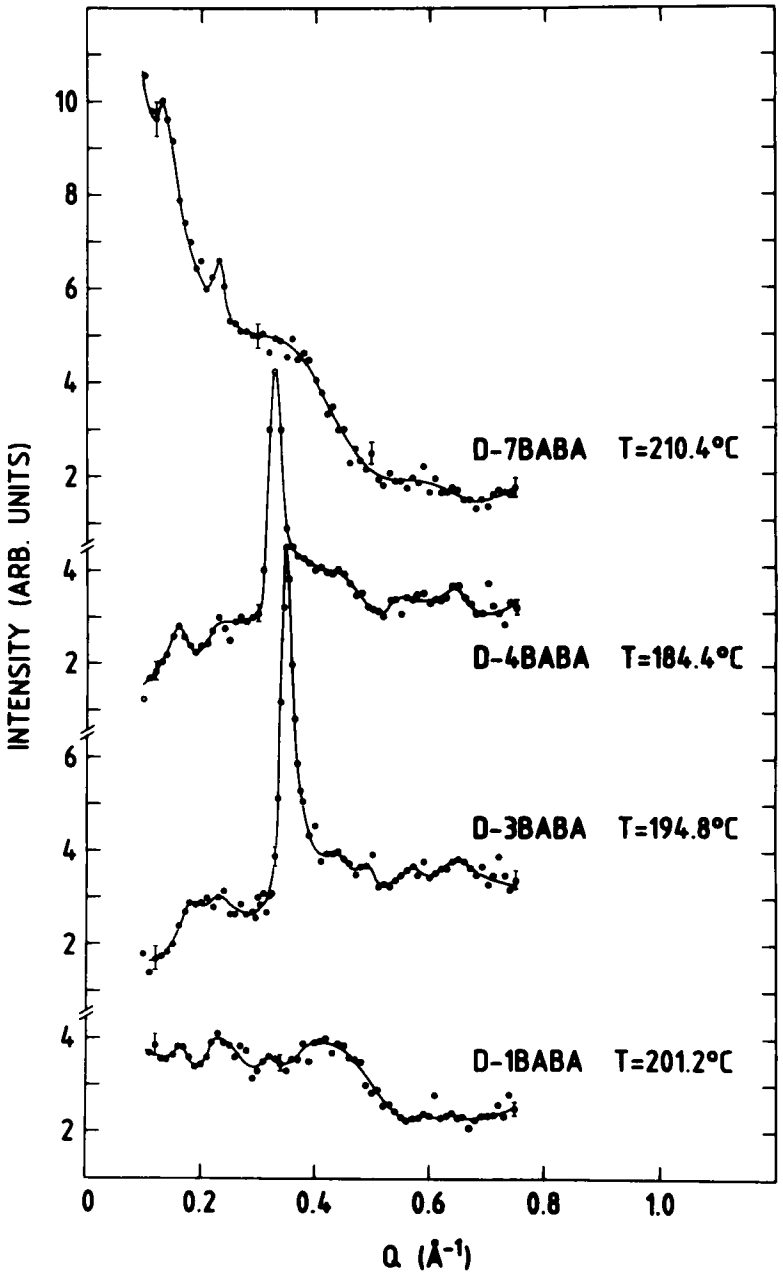

FIGURE 4 Intensity versus $Q_{\parallel}$ ($\vec{Q}\|\hat{n}$) for the meridional scans for D-nBABAs (n = 1, 3, 4, and 7). The intensity has been corrected for background. The lines are visual guides.

the enhanced intensity at small Q values and the broad diffraction maxima seem to indicate that it is a molecular form factor and not the structure factor of a string, that is observed. In 1BABA there is less increase of scattered intensity at small Q and the diffraction peaks are narrower than that of 7BABA, implying a tendency to form 1-d correlated strings. (3) The peak positions for corresponding D- and H-compounds are somewhat different, except for the second order peak. This feature is seen in Figure 5, which shows the distributions for H- and D-4BABA. It can also be seen from Table I, in which the peak positions and the corresponding lattice parameters, obtained using Bragg relations, are listed for the different compounds. The stars in Table I indicate those peaks which are related to the same correlated unit as the 2nd order one. The error in the determination of peak positions could be from 3 to 10 percent for all except the sharp second order peak, whose position has been determined with great accuracy. H-1BABA and H-7BABA were not studied because the corresponding deuterated compounds revealed the absence of 1-d correlation.

The meridional distributions for neutrons and X-rays are surprisingly different. In the X-ray diffraction results, one could easily distinguish the 2nd and 3rd order peaks due to 1-d correlation of dimers. But in the neutron scattering results, only the prominent 2nd order peak is seen while the 3rd order is rarely distinguishable. There is, however, agreement between the X-ray and neutron scattering results as far as values of L_{cu} for $n = 3$ and 4 (Table II), are concerned.

A high temperature scan for D-4BABA is shown in Figure 5, which indicates that at higher temperatures, the structures seen at lower temperatures become less well-defined. The 2nd order peak was studied as a function of temperature for $n = 3$ and 4, in order to obtain the temperature dependence of the correlation length, $\xi_{\|}^{1}$ for the 1-d correlation $\|\hat{\mathbf{n}}$. Figure 6 shows the 2nd order peak in D-3BABA, for various temperatures. It is seen that as the temperature is increased, the intensity of the peak rapidly decreases and it becomes asymmetric with a sharp rise and a slow fall. The latter is due to the presence of a hump on the high Q side of the peak. The intensity of the hump hardly changes with temperature. The half width at half height, $\Delta_L Q$ for the fast rising side of the 2nd order peak does not change much with temperature for $T_{PN} < T < T_{PN} + 30°C$. These characteristics were observed in the case of all 4 compounds. Table III gives ΔQ (the FWHM of the 2nd order peak), $\Delta_L Q$ and the peak intensity as a function of temperature. The errors in determining ΔQ and $\Delta_L Q$ were 5 to 10 percent. The values of ΔQ obtained for the

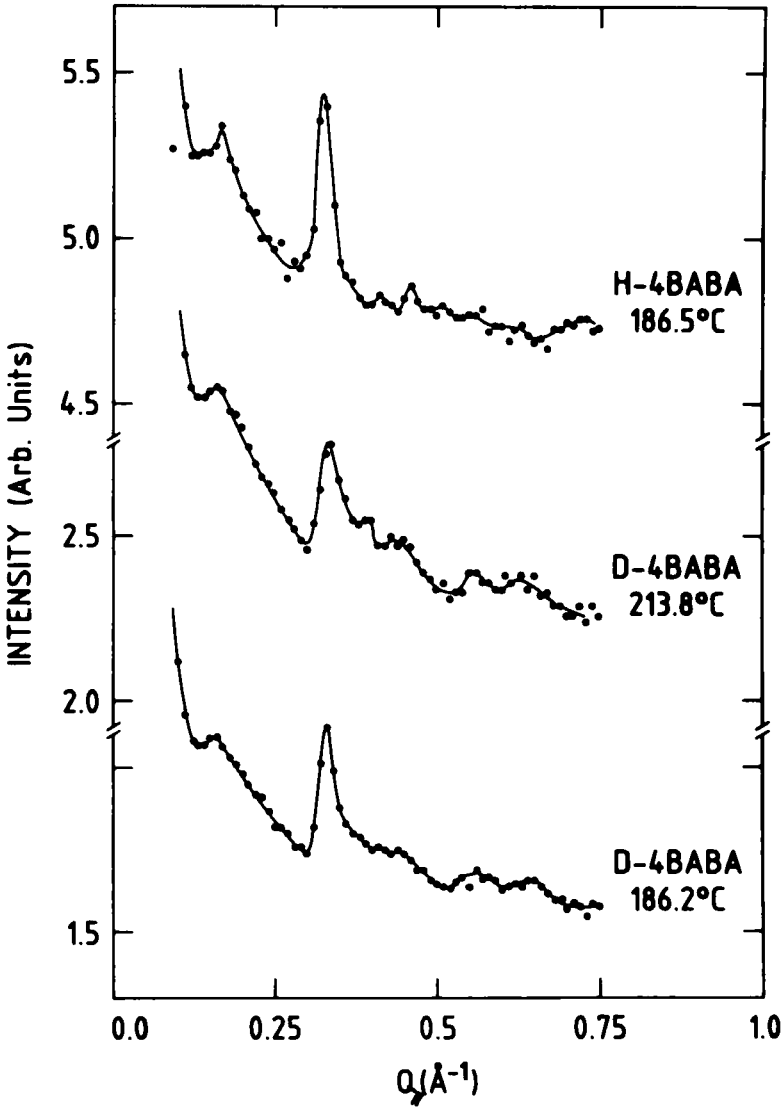

FIGURE 5 Intensity versus $Q_{\parallel}$ for D-4BABA (186.2°C and 213.8°C) and H-4BABA. The lines are visual guides.

TABLE I

Lattice spacings, d, corresponding to the meridional lines.

	D-1BABA		D-3BABA		H-3BABA		D-4BABA		H-4BABA		D-7BABA	
	Q(Å^{-1}) peak	d(Å)	Q(Å^{-1}) peak	d(Å)	Q(Å^{-1}) peak	d(Å)	Q(Å^{-1}) peak	d(Å)	Q(Å^{-1}) peak	d(Å)	Q(Å^{-1}) peak	d(Å)
1	0.170	37.0	*0.180	34.9	*0.180	34.9	*0.160	39.3	0.170	37.0	0.160	39.3
2	0.240	26.2	0.240	26.2	0.280	22.4	0.240	26.2	0.240	26.2	0.230	27.3
3	0.320	19.6	*0.350^{s}	18.0	*0.350^{s}	18.0	*0.330^{s}	19.0	*0.325^{s}	19.4	0.370	17.0
4	0.420	15.0	0.430	14.6	0.440	14.3	0.440	14.3	0.365	17.2	0.590	10.6
5			0.490	12.8	0.530	11.4	0.540	11.6	0.450	14.0		
6			0.570	11.0	0.620	10.1	*0.640	9.8	0.520	12.1		
7			0.650	9.7					0.610	10.3		
8									0.720	8.7		

s: second order line, * peaks related to the same correlated unit as the second order peak.

TABLE II

L_{cu} and $\xi_{\parallel}^{1}$ for 3BABA and 4BABA (both D- and H-) for $T > T_{PN}$.

	D-4BABA	H-4BABA	D-3BABA	H-3BABA
L_{cu} (Å)	38.1	38.7	35.9	35.9
$\xi_{\parallel}^{1}$ (Å)	473.9	539.1	626.0	565.0
$\xi_{\parallel}^{1}/L_{cu}$	12.5	13.9	17.5	16.0
T/T_{NI}	0.84	0.84	0.86	0.86

lowest temperature have been corrected for resolution and $\xi_{\parallel}^{1}$ has been calculated from these using Eq. (1), and is given in Table II. These values are about 2.5 to 3 times that obtained from the X-ray diffraction results. From the present experiments we have $\xi_{\parallel}^{1}(n = 3) > \xi_{\parallel}^{1}(n = 4)$, whereas the X-ray diffraction results indicate $\xi_{\parallel}^{1}(n = 4) > \xi_{\parallel}^{1}(n = 3)$. The reasons for these differences are not clear. No attempt was made to obtain $\xi_{\parallel}^{1}$ from ΔQ at higher temperatures, due to the asymmetric nature of the peak. The values of L_{cu}, obtained from the position of the 2nd order peak are also given in Table II.

The observed temperature dependencies of the intensity and of the width, $\Delta_L Q$, of the 2nd order peak can be interpreted in the following manner. The strings of 1-*d* correlated molecules group together in bundles, for $T \approx T_{PN}$. As the temperature is raised, the strings do not become smaller but the number of strings in the bundle decreases. So the intensity of the 2nd order peak decreases, but its halfwidth, $\Delta_L Q$, remains almost constant up to some higher temperature beyond which it increases. The 1-*d* correlation disappears well below the transition temperature, T_{NI}, as seen from the disappearance of the 2nd order peak, although a tendency to form strings might still exist in the nematic. Thus, the breakdown of 1-*d* correlation would not be responsible for the large values of ΔS_{NI} observed in these compounds. The presence of a hump on the high Q side of the second order peak seems to indicate the following: In the N_F phase, not all the molecules form part of the 1-*d* correlated strings. Some would be in cybotactic groups where such strings are not present, and a few others might not form part of either of these two short range orders. In such a case, the observed meridional ($Q_{\parallel}$) intensity distribution would be a weighted sum of the structure factor of a 1-*d* correlated string along $\hat{\mathbf{n}}$ and the form factor of molecules (both individual ones and those forming part of the cybotactic groups). This would result, respectively, in the sharp 2nd order peak and the hump on the high Q side. The observed hump positions of 4BABAs are not very different from

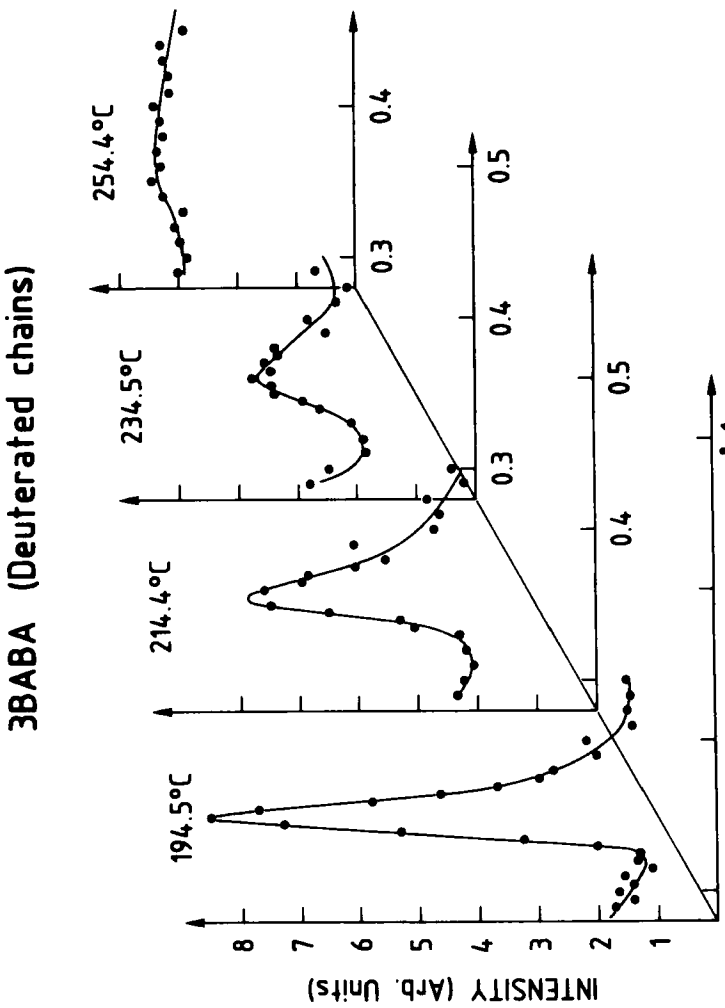

FIGURE 6 Intensity as a function of $Q_{\parallel}$ ($Q_{\perp} = 0$) for the second order meridional line for various temperatures. The lines are visual guides.

TABLE III

Widths and intensities I, of the second order meridional line of 3BABA and 4BABA (both D- and H-), for various temperatures.

H-4BABA				D-4BABA			
T/T_{NI}	ΔQ	$\Delta_L Q$	I	T/T_{NI}	ΔQ	$\Delta_L Q$	I
0.84	0.025	0.0125	6600	0.84	0.028	0.014	5600
0.88	0.031	0.014	3500	0.87	0.030	0.014	4000
0.91	0.041	0.021	2150	0.89	0.038	0.014	2650
0.93	0.031	0.016	1600	0.92	0.038	0.022	1500
				0.94	form	factor	800

H-3BABA				D-3BABA			
T/T_{NI}	ΔQ	$\Delta_L Q$	I	T/T_{NI}	ΔQ	$\Delta_L Q$	I
0.85	0.024	0.012	8300	0.86	0.022	0.011	7200
0.88	0.028	0.014	4250	0.89	0.027	0.010	3400
0.92	0.040	0.024	1950	0.93	0.045	0.014	1600
0.95	0.046	0.026	1450	0.96	form	factor	500

those given by our form factor calculations described below, thus giving support to the above conjecture.

A computer model[7] of the nematic has been constructed to explain the meridional distribution. The compound, 4BABA, was considered. The molecules were assumed to be flat and to have an extended zig-zag conformation. The 1-d string was constructed by placing the molecules at regular intervals, L_{cu}, along the Z-axis (‖ long axis of the molecule). No orientational disorder was taken into account. Neutron cross-sections for the strings were calculated using the following equation:

$$\frac{d\sigma}{d\Omega} = \left| \sum_{n=1}^{N} \exp(i\vec{Q} \cdot \vec{\mathbf{R}}_n) \right|^2 \left| \sum_l b_l \exp(i\vec{Q} \cdot \vec{\mathbf{r}}_l) \exp(-W_l) \right|^2 \quad (2)$$

where R_n = position of the centre of mass of the nth molecule along the string, N = number of molecules in the string, b_l = coherent scattering amplitude of the lth atom in the molecule, r_l its position, and W_l the Debye-Waller factor which we have assumed to be the same for all atoms and equal to $10 \sin^2\theta/\lambda_0^2$ ($= 10Q^2/16\pi^2$).

When $N = 1$, the form factor for the molecule is obtained, while for greater values of N, the structure factor of the string is determined. The form factors for D-4BABA and H-4BABA are shown in Figure

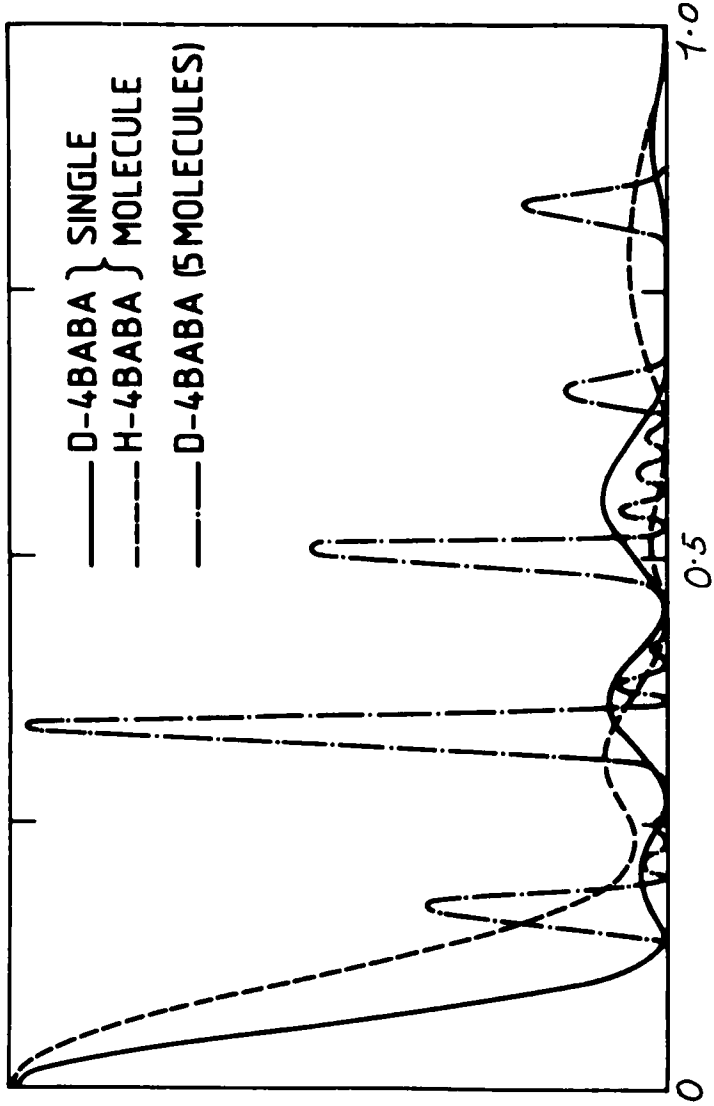

FIGURE 7 Model calculations of neutron cross-sections as a function of $Q_{\parallel}$ ($\vec{Q}_{\perp} = 0$).

7, and they are found to be quite different from each other. The structure factor for $N = 5$, for D-4BABA is also shown in Figure 7. The distribution obtained is different from the one actually observed for D-4BABA. Thus our present model is not a realistic one. To improve the model, it might be necessary to consider molecules which are not flat and to also take into account positional and orientational disorder of the molecules in the string.

c. *Equatorial scan along the 2nd order meridional line* ($\vec{Q} \perp \hat{n}$)

Scans carried out on PAXY along the sharp second order meridional line with $\vec{Q} \perp \hat{n}$ show that for $n = 3$ and 4, the distribution is peaked at $Q_\perp = 0$, at low temperatures ($T \approx T_{PN}$), whereas it is flat at high temperatures. Distributions obtained for D-4BABA at two different temperatures are shown in Figure 8. Although the intensity is poor, the features mentioned above are clearly seen. A rough estimate of the correlation length $\perp \hat{n}(\xi_\perp^1)$ for the strings, can be obtained for $T \approx T_{PN}$ using Eq. (1) and it gives $\xi_\perp^1 \approx 30$ Å. This implies correlation up to fifth neighbours which appears too large. The Ornstein-Zernike correlation function on the other hand leads to, $\xi_\perp^1 \approx 5$ Å, which seems more realistic. Thus these results point to the fact that the number of strings in a bundle decreases as the temperature increases, as was also shown by the results described earlier.

d. *NQES experiments* ($\vec{Q} \perp \hat{n}$)

The results obtained from the NQES experiments were analyzed using the following model.

The observed neutron intensity is due mostly to incoherent scattering from the hydrogen atoms in the molecules. Therefore, the neutron energy spectra would be related to the incoherent part of the scattering law, $S^{inc}(\vec{Q}, w)$. It was assumed that the translational diffusion was too slow to be observed in these experiments and that the vibrational contribution to $S^{inc}(\vec{Q}, w)$ could be neglected. Thus, $S^{inc}(\vec{Q}, w) \approx S_{rot}^{inc}(\vec{Q}, w)$, the rotational part of the scattering law. The rigid and flexible parts of the molecule were assumed to have independent rotational diffusion movements. The rigid part which was defined as consisting of the central rigid portion (see Figure 1) of the molecule and the adjoining methylene groups of the end hydrocarbon chains, was assumed to rotate about the molecular long axis. The flexible part, which consisted of the rest of the end chains, was pictured as rotating about the hydrocarbon chain axis. The rotational movement of both parts was assumed to involve random walk

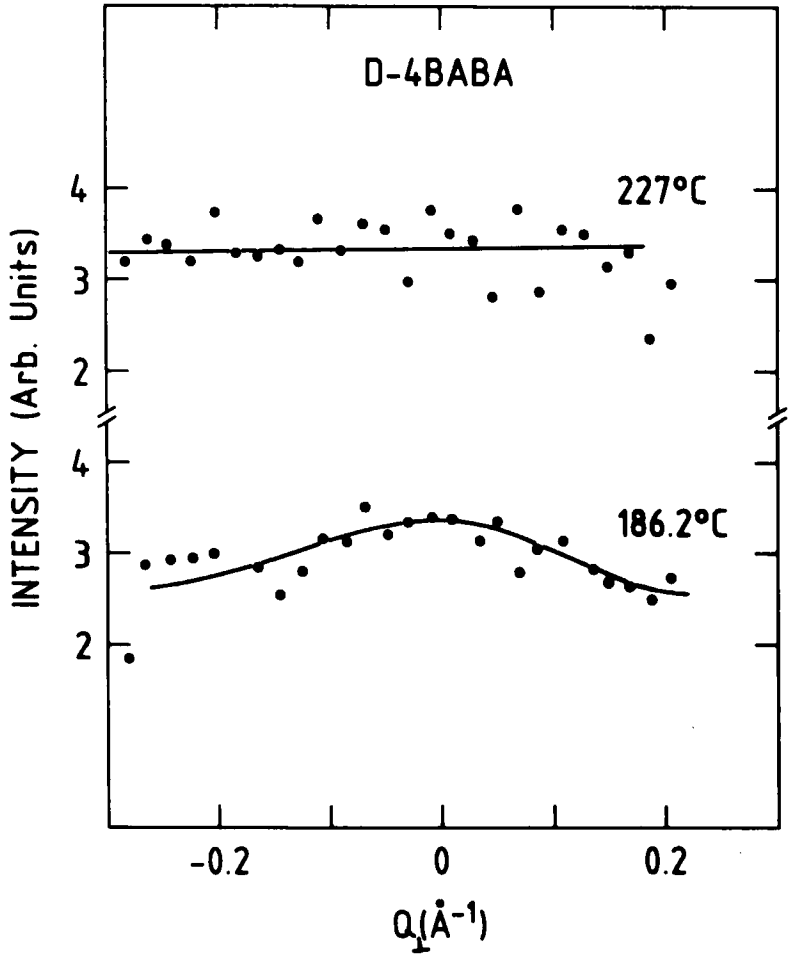

FIGURE 8 Intensity versus $Q_\perp$ ($\vec{Q}_\parallel \neq 0$) for the second order meridional line of D-4BABA at 186.2°C and 227°C. The lines are visual guides.

of H atoms among N equidistant sites.[8,9] N was taken to be equal to 6 since, in the nematic phase, the packing of molecules $\perp \hat{\mathbf{n}}$, would be hexagonal at short range. The scattering law for such a movement is given by[8,9]

$$S^{inc}(\vec{\mathbf{Q}}, \omega) = f(Q, a, \vartheta, \tau, \omega)$$

$$= A_0(Qa \sin\vartheta)\delta(\omega) + \frac{1}{\pi}\sum_{n=1}^{N} A_n(Qa \sin\vartheta)\frac{\tau_n}{1 + (\omega\tau_n)^2}, \quad (3)$$

where

a = the radius of gyration,

ϑ = angle subtended by $\vec{\mathbf{Q}}$ with the axis of rotation,

$$A_n(x) = \frac{1}{N}\sum_{\rho=1}^{N} J_0\left(2x \sin\frac{\pi p}{N}\right)\cos\left(\frac{2\pi pn}{N}\right)$$

and

$$\tau_n = \tau_1 \frac{\sin^2\pi/N}{\sin^2 n\pi/N}.$$

The observed intensity, $I(\vec{\mathbf{Q}}, \omega)$ can be written as,

$$I(\vec{\mathbf{Q}},\omega) \propto \left[\sum_{j}^{rigid} S_j^{inc}(\vec{\mathbf{Q}},\omega) + \sum_{i}^{flexible} S_i^{inc}(\vec{\mathbf{Q}},\omega)\right] \tag{4}$$

$$= \left[\sum_{j}^{rigid} f(Q,a_j,\vartheta_r,\tau_1^r,\psi) + \sum_{i}^{flexible} f(Q,a_i,\vartheta_f,\tau_1^f,\omega)\right]. \tag{4a}$$

$\sum^{rigid}$ and $\sum^{flexible}$ are summations over the hydrogen atoms in the rigid and flexible parts of the molecule, respectively. Eq. (4) was fitted to the observed spectra. It did not give a good fit to our results, unless either (a) the background was increased to a value greater than that observed experimentally, or (b) an additional Lorentzian term with a large energy width ($\approx$0.5 THz) was added to the right hand side of Eq. (4). The values of relaxation times obtained, using these two modifications of Eq. (4) are hardly different. In the following, we refer to the results obtained by fitting Eq. (4) to our data, modified as in (b), that is,

$$I(\vec{\mathbf{Q}}, \omega) \propto A\left[\sum_{j}^{rigid} f(Q, a_j, \vartheta_r, \tau_1^r, \omega) + \sum_{i}^{flexible} f(Q, a_i, \vartheta_f, \tau_1^f, \omega)\right] + B\left(\frac{\tau_L}{1 + (\omega\tau_L)^2}\right] \tag{5}$$

where A and B are constants and $1/\tau_L$ is the Lorentzian width ($\approx 2\pi \times 0.5 \times 10^{12}$ radians/sec.). A, B, τ_L, τ_1^r and τ_1^f were used as param-

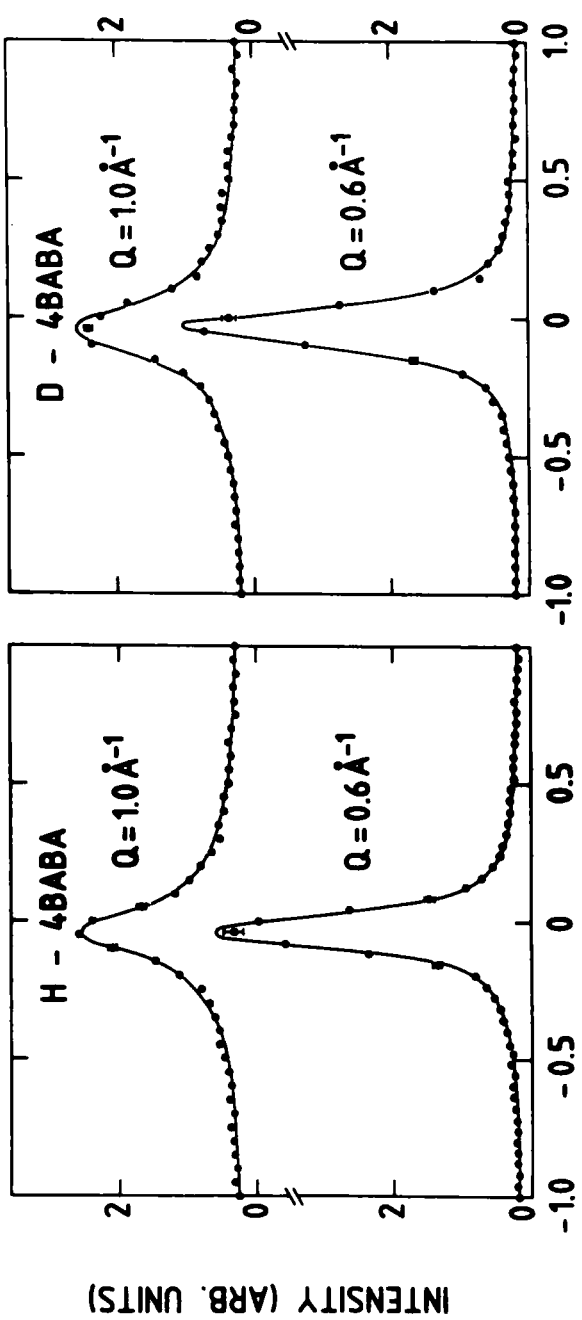

FIGURE 9 Intensity as a function of ω for D-4BABA for $Q = 0.6$ Å^{-1} and 1.0 Å^{-1}. The points are experimental points and the lines represent best fit of Eq. (5) to our results.

eters while fitting Eq. (5) to our data. For D-4BABA, since there were no hydrogen atoms in the flexible part, the contribution of the second term of Eq. (5) was nil. Hence, of the two rotational relaxation times, only τ_1^r was obtained by fitting the data for D-4BABA. While fitting the H-4BABA spectra, the value of τ_1^r was constrained to be equal to that obtained for D-4BABA for the same values of Q and temperature, so that τ_1^r was not a parameter used in fitting. τ_1^f was obtained in this case. Figure 9 shows the observed energy spectra for the two compounds and the curves calculated using the parameters obtained for the best fit, for $T = 186°C$. It is found that the agreement between the calculations and the experimental results are fairly good. Table IV gives the values of τ_1^r and τ_1^f obtained for the best fits. The following interesting points can be seen: (1) τ_1^r and τ_1^f vary with varying Q showing that the model used is not a good one. (2) τ_1^f is not very different from τ_1^r but it varies less with Q than τ_1^r does. (3) Neither τ_1^r nor τ_1^f vary much with increasing temperature, indicating that the two rotational movements are not influenced much by the 1-d correlation of molecules. If they were affected, τ_1^r and τ_1^f would have decreased considerably for T increasing from 186°C to 221°C, due to the accompanying large decrease in the 1-d correlation strength observed in the diffraction experiments.

The failure of the model to explain our results could be related to certain factors. The translational diffusion motion that we have neglected to consider might not be as slow as we assumed. This motion might have to be taken into account if the value of the transitional diffusion coefficient, $D_\perp(\perp\hat{\mathbf{n}})$, is sufficiently large, as seems to be the case in some nematics.[10] If this be the reason for the observed Q-dependence of τ_1^r and τ_1^f, their values obtained for $Q = 0.6\ \text{Å}^{-1}$ would be nearer to the true values of the relaxation times. The small, though finite contribution of the broad Lorentzian term of Eq. (5) could be due to our not taking into account some fast molecular motion.

CONCLUSIONS

The results of our diffraction studies with nBABAs have shown the following: (a) 1-d correlation of molecules is weak for $n = 1$ and negligible for $n = 7$, but is strong for $n = 3$ and 4. (b) The strength of the 1-d correlation breaks down very fast with increasing temperature. This breakdown is not brought about by the decreasing number of molecules correlated along $\hat{\mathbf{n}}$, but by having lesser number of strings of correlated molecules. (c) There is a large difference between the

TABLE IV

Relaxation times, τ_1^r and τ_1^f as a function of Q and temperature for D-4BABA and H-4BABA.

Sample	D-4BABA				H-4BABA			
T (°C)	186.0		221		186.0		221	
Q (Å^{-1})	0.6	1.0	0.6	1.0	0.6	1.0	0.6	1.0
τ_1^r (10^{-11}s)	2.24 ± 0.09	0.683 ± 0.041	1.43 ± 0.04	0.410 ± 0.029	2.24	0.683	1.43	0.410
τ_1^f (10^{-11}s)	—	—	—	—	0.925 ± 0.091	0.720 ± 0.072	0.860 ± 0.084	0.536 ± 0.079

X-ray and neutron diffraction results, both as regards structure related to 1-*d* correlation as also concerning the 1-*d* correlation length, $\xi_{\parallel}^{1}$, which is much larger in the case of the present experiments.

The NQES results show that (1) the rotational diffusion model that we have used does not describe well the molecular dynamics, and (2) the rotation diffusion of the rigid and flexible parts of the molecule are not very affected by the 1-*d* correlation.

Acknowledgments

We are very thankful to A. J. Dianoux and B. Hennion for useful discussions. We would like to thank M. Lambert for helpful suggestions and A. V. Patankar for preparing some of the compounds for us. We are also thankful to J. Mons and J. P. Beauchef for technical help.

References

1. A. S. Paranjpe, K. Usha Deniz, V. Amirthalingam, and K. V. Murlidharan, *Proceedings of the Nuclear Physics and Solid State Physics Symposium*, Delhi (1980).
2. A. De Vries, *Liquid Crystals*, Ed. S. Chandrasekhar (Pramana Supplement, 1974).
3. K. Usha Deniz, E. B. Mirza, P. S. Parvathanathan, A. V. Patankar and A. S. Paranjpe, *Mol. Cryst. Liq. Cryst.*, (to be published).
4. L. V. Azaroff, *Mol. Cryst. Liq. Cryst.*, **60**, 73 (1980).
5. L. V. Azaroff, *Elements of X-ray Crystallography*, (McGraw-Hill Book Co., Inc., New York, 1968), pp. 551.
6. L. S. Ornstein and F. Zernike, *Proc. Sect. Sci. K. med. Akad. Wet.*, **17**, 793 (1914).
7. The values of the bond lengths and bond angles used in constructing the model were given to us by J. Doucet.
8. A. J. Dianoux, F. Volino and H. Hervet, *Mol. Phys.*, **30**, 1181 (1975).
9. J. D. Barnes, *J. Chem. Phys.*, **58**, 5193 (1973).
10. G. J. Kruger, *Phys. Rep.*, **82**, 230 (1982).